

2(m x)

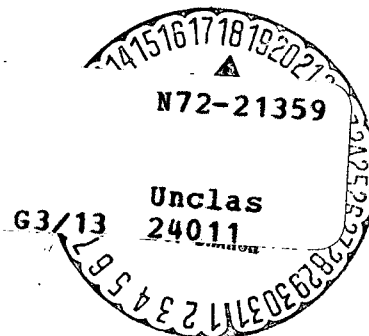
NASA TECHNICAL TRANSLATION

NASA TT F-14,215

STUDY ON SAND MOVEMENT BY WIND

R. Kawamura

(NASA-TT-F-14215) STUDY ON SAND MOVEMENT
BY WIND R. Kawamura (Scientific
Translation Service) Apr. 1972 48 p
CSCL 08M



Translation of "Hisa no kenkyū". Tōkyō Daigaku
Rikōgaku Kenkyūsho Hōkoku (Reports of Physical
Sciences Research Institute of Tokyo University),
Vol. 5, No. 3 - 4, Oct., 1951, pp. 95-112.

NATIONAL AERONAUTICS AND SPACE ADMINISTRATION
WASHINGTON, D.C. 20546 APRIL 1972

Reproduced by
NATIONAL TECHNICAL
INFORMATION SERVICE
U S Department of Commerce
Springfield VA 22151

CAT. 13 48

STUDY ON SAND MOVEMENT BY WIND

R. Kawamura

ABSTRACT. Sand movement by wind is studied in detail in this paper. The effect of wind turbulence on sand particles is neglected by taking into account their susceptibility in the natural wind. Sand particles move downstream with bouncing motions near the sand surface and in the stationary state they gain on an average as much momenta from the wind as they lose at the moment of collision on the sand surface. From this, the relation between the rate of sand flow quantity and the friction velocity of the wind is derived, which agrees very well with the experimental results in the wind tunnel and field. The statistical treatments of the phenomena make it possible for us to calculate the vertical distributions of density of sand particles and quantity of sand flow, which again coincide completely with experiments. It becomes clear in this study that the mass of moving sand increases more rapidly in the lower layer than is given in the ordinary diffusion theory. (Received July 19, 1951)

1. INTRODUCTION

/95*

Various research has been performed thus far concerning the movement of sand by the wind. The main streams in this research are the theories of Exner [1] and the theories of Bagnold [2, 4]. Whereas Exner regards the phenomena of flying sand as a sort of diffusion phenomenon caused by air turbulence, Bagnold concludes from the results of observing flying sand movement that the effects of the wind on the sand grains can be omitted and treats the grains of sand as projectiles. As important results from these theories, we might mention that Exner obtained the distribution of flying sand

* Numbers in the margin indicate the pagination in the original foreign text.

in terms of height, while Bagnold was able to determine the relationship between the wind velocity and the total quantity of flying sand. However, neither of them was able to obtain the results of the other, nor were they able to explain completely the experimental results in terms of their results. For this reason, a more universally valid theory is required. The present writer has been engaged in research on flying sand from this standpoint, and the present paper is a summary of his research results. This research deals with the fundamental questions of the flying sand phenomenon, and the various conditions are considered in extremely simplified terms. However, with a few corrections, it can be applied to actual problems of erosion control or of transport of powdered grains by a liquid.

2. PHYSICAL PROPERTIES OF SAND GRAINS AND THE SAND SURFACE

Individual grains of sand have entirely different sizes. The usual method for seeking the size distribution of sand grains is to sift sand samples with sieves having different meshes and to measure their weights. Figure 1 is an example of this cited from Bagnold's monograph [3]; $\phi(d)$ indicates the weight distribution of sand grains having a size of d . This sand is the so-called dune sand. The characteristic feature of Figure 1 is the sharp

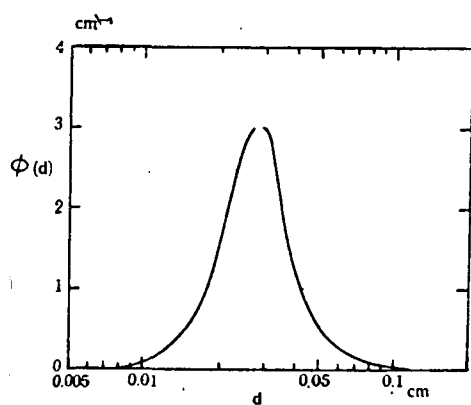


Figure 1. Grain diameter distribution of dune sand.

concentration of the distribution curve in the vicinity of $d = 0.3$ mm. There are extremely few sand grains with d of less than 0.1 mm or more than 0.6 mm. This tendency is commonly seen in dune sand with intense flying sand movement by the wind. We already have Bagnold's research concerning its causes [3]. In this research also, we deal with dune sand with an average grain diameter

of 0.2 - 0.3 mm. The specific gravity of the individual grains of sand is not constant, but the average is about 2.5, and there are almost none with a

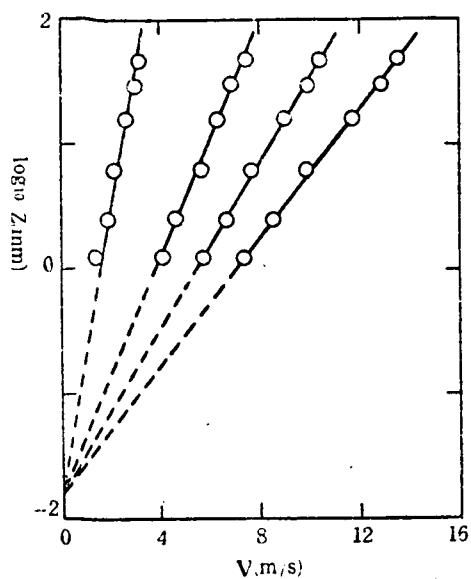


Figure 2. Wind velocity distribution in vicinity of sand surface (no flying sand)

specific gravity less than 2.4 or more than 2.7. In this monograph, grains of sand will be discussed by analogy with a sphere having the same volume.

Next, let us describe the properties of the sand surface. In a natural state in sandy beaches or deserts, the sand surface is not flat. In addition to unevenness due to the sand grains, the sand surface assumes the form of various large and small wave patterns, ranging from sand ripples with a height of several mm to large-scale sand dunes, with a height of 50 m

or more. However, in this monograph, because of the necessity of having a fundamental treatment of the sand movement, the sand surface was considered to be flat. When considering the length, it is inevitable that there should be a certain vagueness, of the same order as the size of the sand grains. The ratio between the sand density in the vicinity of the sand surface σ_s and the real density of the sand grains σ , $\lambda = \sigma_s / \sigma$, is called the volume ratio, and the concentration of the sand grains is expressed in terms of λ . It is quite difficult to measure λ , but there is a value of approximately 0.45 in the vicinity of the sand surface in the natural state. Exner states that he obtained a value of $\sigma_s = 1.22 \text{ g/cm}^3$, although the measurement method is not clear.

3. PROPERTIES OF THE WIND IN THE VICINITY OF THE GROUND LEVEL

There are numerous theoretical equations and experimental equations for expressing the wind velocity distribution in terms of height in the vicinity of the ground level; the divergences are due to the boundary layer. In

relatively flat places with no obstacles, such as sandy plains, it is most convenient to use Prandtl's Equation [5]. The experiments of the writer and colleagues show that these values coincide well with the experimental values to a height of several meters above the ground. According to this equation, the wind velocity $V(z)$ at a height z above the ground level is expressed as follows

$$V(z) = 5.75 \rho V_\tau \log_{10} \frac{30z}{k} \quad (3.1)$$

Here, ρ is the density of the wind, and V_τ is the variable called the friction velocity. If τ_0 is the friction stress operating on the surface, V_τ is defined in the following terms:

$$V_\tau = \sqrt{\tau_0 / \rho} \quad (3.2)$$

Also, k is called the coarseness of the surface; this is a quantity having a length dimension related to the unevennesses present in the surface. In flat sand surfaces, it is considered to be about the same size as the sand grains. Figure 2 shows the wind velocity distribution, as sought by means of a Pitot tube, in a layer extremely close to the sand surface. The sand was spread out on the floor of a wind tunnel with a height of 80 cm and a width of 5 cm; after the surface was leveled out, the sand was moistened with water so that the sand grains would not be moved by the wind. As is clear from the results, Prandtl's logarithmic law (3.1) is almost perfectly satisfied. The wind velocity distribution of natural winds obtained in outdoor experiments also displays approximately the same results in the vicinity of the ground level, and $V(z)$ and $\log z$ are in direct proportion to each other. If the linear relationship between $V(z)$ and $\log z$ is sought from experiments about the wind velocity distribution, it is possible to use (3.1) and to find V_τ from this gradient. Consequently, the friction stress τ_0 of the sand surface can be sought from (3.2).

There is a turbulence called "gust" of wind in natural wind. The wind velocity is constantly fluctuating in the region of the mean value. Taylor [6] discovered a method to seek the distribution of the turbulence energy (the turbulence spectrum) with respect to the frequency (number of oscillations) from long-term records of the wind velocity variations at a single point. The writer applied this method to the wind in the vicinity of the ground and sought the turbulence spectrum of natural wind. An example of this is given in Figure 3, which gives the results for cases when the wind velocity is

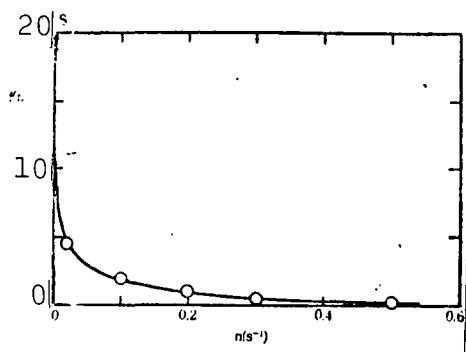


Figure 3. Wind turbulence spectrum.

5 m/s. In this figure, $f(n)dn$ represents the energy distribution of the fluctuating wind velocity in which the frequency is between n and $n + dn$. As is clear from this figure, in natural wind there is an extremely small percentage of the energy in the part with a large frequency, and in the range where $n > s^{-1}$, $f(n)$ may be considered to be almost zero.

/97

4. SUSPENSION OF SAND GRAINS IN THE AIR

When a sphere with a diameter d moves in a straight line through a fluid at a speed U , the force of resistance W to which the sphere is subjected follows Stokes' law [7] as long as the Reynolds number is small. That is,

$$W = 3\pi\mu U d \quad (4.1)$$

Here, μ represents the viscosity coefficient of the fluid. Equation (4.1) applies when the Reynolds number $R = Ud/(\mu/\rho)$ (ρ is the density of the fluid) is less than 1. In cases when grains of sands are moving through the air, the R number is considered to be more or less within the range of zero to about 50; this goes beyond the range of application of Equation (4.1).

However, no one has obtained a law of resistance applicable over such a broad

range, and experiments indicate that in R numbers of this range the resistance clearly varies in a range closer to the first power of the speed than to the second power. Therefore, in this monograph, Equation (4.1) is applied in an approximate fashion. The next problem is the difference in resistance between sand grains having complicated shapes and spheres with identical volume. As is clear from the experimental results in the past, not a very great difference is seen [8]. Besides, there are other questions such as the problem of unsteady motion and the problem of the effects of the boundary walls [8], but in order to simplify the procedure, in this monograph the sand grains are replaced by spheres of identical volume, and it is assumed that they are subjected to resistance as given in (4.1) during movement.

The origin of the coordinates is located on the sand surface. The x axis is plotted in the main wind direction; the z axis — in the vertical direction, and the y axis — at 90 degrees to them. If the momentary values of the wind velocity in each direction are expressed as V_x , V_y , and V_z , the mass of the grains of sand as m, and the time as t, the three-dimensional equation of motion will be as follows

$$m \frac{d^2x}{dt^2} = 3\pi\mu d \left(V_x - \frac{dx}{dt} \right) \quad (4.2)$$

$$m \frac{d^2y}{dt^2} = 3\pi\mu d \left(V_y - \frac{dy}{dt} \right) \quad (4.3)$$

$$m \frac{d^2z}{dt^2} = 3\pi\mu d \left(V_z - \frac{dz}{dt} \right) - mg \quad (4.4)$$

However, the forces to which the grains of sand were subjected by the pressure gradient in the air can be omitted since d has such a small value.

In (4.4), if we set $w = dz/dt$, we obtain

$$\begin{aligned} \frac{dw}{dt} + \beta w &= \beta V_z - g, \\ \beta &= 3\pi\mu d/m \end{aligned} \quad (4.5)$$

The quantity V_z represents the momentary wind velocity in the z direction, and it is possible to expand this in a Fourier series with respect to time. Since (4.5) is linear, it will be sufficient to consider one term in it.

Setting

$$V_z = V_{zn} \sin 2\pi nt$$

let us seek a solution for (4.5). We obtain the following:

$$v = A_0 e^{-\beta t} - \frac{g}{\beta} + \frac{V_{zn}}{\sqrt{1 + (2\pi n/\beta)^2}} \sin(2\pi nt - \alpha), \quad \alpha = \tan^{-1}(2\pi n/\beta) \quad (4.6)$$

A is an integration constant. The first term of this equation is a damping term and is not very important. The second term represents the final dropping speed of the grains of sand, and the third term represents the influence of wind turbulence on the grains of sand. The meaning of the third term is that, when the wind velocity changes, the speed of the grains of sand also changes, but the amplitude of the latter has the relation $1/\sqrt{1 + (2\pi n/\beta)^2}$ towards the amplitude of the wind velocity, and the phase of the oscillations lags behind by α . This amplitude ratio varies as a function of β and n . Taking into consideration a situation in which the grains of sand move through the air, if it is assumed that $d = 0.25$ mm and σ (the density of the sand grains) = 2.5 g/cm^3 , we will obtain a value of $\beta = 2.08 \text{ s}^{-1}$, and the amplitude ratio will be less than 0.07 at $n > 5 \text{ s}^{-1}$. If the wind velocity in the vicinity of the ground is 5 m/s, and if V_{zn} is assumed to be 20% of it — that is, 1 m/s — the third term will be less than 0.07 m/s if $n > 5 \text{ s}^{-1}$. On the other hand since the value of g/β will reach 5 m/s in sand grains of this size, in cases where there is a large value of n , it will be possible to omit the third term of (4.6) more readily than the second term. That is, one may assume that slight wind turbulence has no effect on the movement of sand.

Next, in cases where there is a small value of n , the amplitude ratio will approach 1. Furthermore, since the energy distribution of wind turbulence $f(n)$ is greater, the smaller is n , the second and third terms of (4.6) will be about the same size. However, on the other hand, most of the movement of flying sand takes place in layers close to the sand surface, and it is rare for sand to reach an altitude of more than 30 cm above the sand surface. In

view of the dropping speed g/β and this altitude, it is no doubt appropriate to assume that a time of only about 0.2 seconds would be necessary for the grains of sand to fly up from the ground level and to return to the ground level. Consequently, wind turbulence with a period greater than this would no longer be turbulence, for the grains of sand; rather, it would merely appear that there were changes in the mean wind velocity at the time. In other words, turbulence with a period longer than the time that the grains of sand are in the air would not have the capacity to diffuse the sand. Consequently, it is possible to omit turbulence with a small number of oscillations in the sense of suspending grains of sand in the air.

On the basis of the arguments given above, one may conclude that wind turbulence has no diffusion capacity for dune sand, which is the type of sand discussed in this monograph. Consequently, it may be said that Exner's diffusion theory is not valid.

As mentioned above, the suspension of the grains of sand is related solely to the size of β . Since β is in inverse proportion to d^2 , the suspension properties increase rapidly, the smaller is the grain diameter.

5. BEGINNING OF SAND GRAIN MOTION AND ITS CONDITIONS

A grain of sand located in the upper layer of the sand surface and directly exposed to the wind remains stationary as long as the wind velocity is below a certain value, but it begins to move when the wind velocity goes beyond this. The wind velocity at this time is called the limiting wind velocity. A great deal of research has been done thus far about this limiting wind velocity. Jeffreys [9] and Davis [10] thought that objects exposed to wind were subjected to buoyancy caused by the wind pressure. They assumed that the objects begin to move when this buoyancy balanced off the weight of the objects. They gave the limit wind velocity V_c in the following form.

$$V_c = \text{const} \sqrt{\frac{\sigma - \rho}{\rho} g d} \quad (5.1)$$

Here, σ and ρ are the density of the object and of the fluid, and d is the size of the object. (5.1) coincides well with the experimental results with respect to the relationship between V_c and d , but, on the other hand, White [11] reports his experiments stating that such a lift did not exist in grains of sand placed on the sand surface. Consequently, (5.1) must be derived without assuming any lift.

First, let us assume that N grains of sand are included per unit volume in the vicinity of the sand surface. In this case, the real volume of the grains of sand here will be $N\pi d^3/6$. When we use the volume ratio λ , we obtain $N = 6\lambda/\pi d^3$. As for the number of grains of sand located on the sand surface and directly exposed to the wind, if we assume that n is the average number per unit of area, we obtain:

$$n = V^{2/3} = (6\lambda/\pi)^{2/3} / d^2 \quad (5.2)$$

A friction stress τ_0 derived from the wind operates on the sand surface, but it is possible to assume that most of this force operates on the sand surface in the form of the resistance to which the n grains of sand (protruding on the sand surface) are exposed. Consequently, the mean value of the resistance on one grain of sand, D , may be expressed as follows:

$$D = \frac{\tau_0}{n} = \rho \left(\frac{\pi}{6\lambda} \right)^{2/3} d^2 \tau_*^2 \quad (5.3)$$

In order for the grain of sand to begin to move, it is necessary for the force operating on the grain of sand to overcome the static friction. Consequently, we obtain the following equation as the condition for most of the grain sands at the sand surface to begin to move

$$D \geq mg \tan \varphi_0 \quad (5.4)$$

Here, ϕ_0 represents the static friction angle of the sand surface. If the limiting frictional velocity when the sand grains begin to move is expressed as V_{tt} , we obtain the following from the above two equations:

$$V_{tt} = \left(\frac{\pi}{6} \right)^{1/6} \lambda^{1/3} (\tan \phi_0)^{1/2} \sqrt{\frac{\sigma - \rho}{\rho} g d} \quad (5.5)$$

Since according to (3.1) there is a directly proportional relationship between V_{tt} and the wind velocity at a certain altitude, both (5.1) and (5.5) express the same conditions. That is, it has been possible to explain the experimental results without assuming a lift. Comparing the experimental results sought by Chepil [12] and the theoretical value from (5.5), we find that the value of V_{tt} obtained by the latter is several times greater than the experimental value. However, while the value of V_{tt} obtained with (5.5) indicates the average value for many grains of sand, there is a tendency in experiments to observe more readily the V_{tt} for the grains of sand which move most easily. Therefore, it is only natural that a value so much smaller than the theoretical value should be obtained.

In wind tunnel experiments using sand with an average grain diameter of 0.25 mm and $\sigma = 2.5 \text{ g/cm}^3$, the writers obtained a value of $V_{tt} = 23.4 \text{ cm/s}$. This value coincides well with the results of Chepil.

6. MOVEMENT OF GRAINS OF SAND IN THE AIR

Well dried sand was spread out to a thickness of about 5 cm on the floor in the above-mentioned wind tunnel. Wind was blown over it, and the movement of the sand was observed. If one focuses attention on single grains of sand, they begin to move as soon as the wind velocity reaches a certain value. First of all they almost roll over the sand surface. Gradually the speed is accelerated, and when they move several centimeters they suddenly fly up in the air. In the air, they describe a sort of parabola and again drop down onto the sand surface. After colliding with the sand surface,

it is difficult to determine whether the same grain of sand jumps up again or whether it impels other grains into motion. At any rate, as a whole, this jumping motion is repeated again and again. The distance of a single flight and the highest altitude both vary depending upon the wind velocity, but they are more or less on the order of several centimeters. Of course, in rare instances there are some grains of sand moving at altitudes of 10 cm or more, but these amount to only a small percentage of the whole. When illuminated by strong rays of light, the flight route of the grains of sand becomes clear. However, in this case the scattered light from the grains of sand differs with each succeeding moment, and the flight route sometimes appears to be a dotted line. This phenomenon obviously indicates that the grains of sand are engaging in rotational motion in the air. It is more difficult to observe this in outdoor experiments than in a wind tunnel, but similar observations can be performed by placing one's eyes near the sand surface. In this case also the movement of the grains of sand is essentially the same as that inside the wind tunnel. The flight course of the sand grains describes a parabola, and there is absolutely nothing resembling the phenomenon of suspension in the air due to the effects of wind turbulence. /99

Based on the above-mentioned observation results and the suspension of grains of sand discussed in Section 4, let us determine the movement of the sand grains in the air, omitting the influence of wind turbulence on the flying sand movement and considering only the mean wind velocity. If we assume that the mean wind velocity V is constant, the equation for the movement of grains of sand will be the same as for $V_x = V$, $V_y = V_z = 0$ in (4.2), (4.3), and (4.4). If we locate the point of origin at the point where the grain of sand jumps out, and if we adopt initial conditions of $dx/dt = u_1$, $dy/dt = v_1$, and $dz/dt = w_1$ when $t = 0$, the solution of the movement equation will be as follows:



$$\begin{cases} x = (-V + u_1)(1 - e^{-\beta t})/\beta + Vt, \\ y = v_1(1 - e^{-\beta t})/\beta, \\ z = (w_1/\beta + w_1)(1 - e^{-\beta t})/\beta - gt/\beta. \end{cases}$$

If the movement of the grains of sand occurs at an extremely low altitude, and consequently if one jump has a short lifetime, it will be possible to set $\beta t \ll 1$, and the above equations can be written approximately in the following manner.

$$x = u_1 t + \beta(V - u_1)t^2/2, \quad (6.1)$$

$$y = v_1 t, \quad (6.2)$$

$$z = w_1 t - (1 + \beta w_1/g)gt^2/2 \quad (6.3)$$

Furthermore, since $\beta w_1/g$ is considered to be smaller than 1 (6.3) will be as follows:

$$z = w_1 t - gt^2/2 \quad (6.4)$$

In the final analysis, as long as the flying sand movement takes place in the low layers near the sand surface, it is permissible to omit the air viscosity with respect to movement in the y and z directions.

The speeds in the three directions u, v, and w may be expressed in the following manner using z

$$u = u_1 + \frac{\beta(V - u_1)}{g} w_1 \left(1 \pm \sqrt{1 - \frac{2gz}{w_1^2}} \right), \quad (6.5)$$

$$v = v_1,$$

$$w = \pm w_1 \sqrt{1 - \frac{2gz}{w_1^2}}. \quad (6.6)$$

$$(6.7)$$

The upper signs in the formulas represent the values for the grains of sand while they rise, and the lower signs represent their values while they come down.

If we add 2 to the values during dropping, we obtain the following:

$$\begin{cases} u_2 = u_1 + 2\beta(V - u_1)w_1/g \\ w_2 = -w_1 \end{cases} \quad (6.8)$$

If L represents the flight distance, T the flight time, and h the maximum height of arrival of the grains of sand (let us call this the flight height),

the following expression can be adopted:

$$\begin{cases} J = 2 \left[\frac{u_1 w_1}{g} + \frac{\beta(V-u_1)}{g^2} w_1^2 \right], \\ T' = 2w_1/g, \\ h = w_1^2/2g, \end{cases} \quad (6.9)$$

7. ACCELERATED FLYING SAND FLOW

Let us consider a case when the wind blows over a broad surface of dry sand. When the wind velocity rises above the limiting value, the grains of sand at the windward side of the sand surface will be unable to withstand the forces emanating from the wind and will begin to move. These grains of sand will collide with the sand surface, destroy the stability of the sand surface, and induce flying sand movement in rapid succession. Therefore, the amount of flying sand will gradually increase. However, when there is an increase in the amount of flying sand, the momentum taken away by the grains of sand will increase, and therefore it is possible that the wind velocity will weaken inside the flying sand layer. Consequently, the amount of flying sand, rather than increasing infinitely, will rather reach a certain saturation point at a point far enough downwind.

Let us use G to represent the mass of sand dropping down per unit area on the sand surface per unit time, G' — to represent the sand which at this time does not resume jumping but settles down on the sand surface, and G'' — to represent the sand which begins to move anew because of the wind. Naturally, G' is in direct proportion to G . The friction stress of the wind is connected with G'' , and G'' is zero at a stress less than the limiting friction stress. Taking into consideration the points mentioned above, let us assume the following hypotheses:

$$G' = aG, \quad G'' = b(\tau_w - \tau_l) \quad (7.1)$$

Here, τ_w and τ_t represent, respectively, the stress of the wind on the sand surface, and the limiting stress. Quantities a and b are constants.

In cases where flying sand flow is present, the friction stress τ_0 operating on the sand surface can be divided into two parts: τ_s , that due to collision of the sand grains, and τ_w , that due to direct wind

/100

$$\tau_0 = \tau_s + \tau_w \quad | \quad (7.2)$$

Since τ_s naturally is in direct proportion to G , we can set the following:

$$\tau_s = cG \quad | \quad (7.3)$$

On the other hand, let us assume that L is the mean flying distance of the grains of sand and assume that approximately all grains of sand have the same flying distance. In this case, the grains of sand which have jumped from point $x = x$ will drop down at point $x + L$. Therefore,

$$G(x+L) = G(x) - G'(x)L + \frac{1}{2}G''(x)L^2 \quad |$$

If we assume that L is small, we obtain:

$$\frac{dG}{dx} = \frac{1}{L}(-G' + G'') \quad | \quad (7.4)$$

If we insert (7.1), (7.2) and (7.3) into (7.4), we obtain the following differential equation.

$$\frac{dG}{dx} = \frac{1}{L} \left[b(\tau_0 - \tau_t) - (bc + a)G \right] \quad | \quad (7.5)$$

If $x = 0$ and $G = 0$, the solution for (7.5) will be the following

$$G = \frac{b(\tau_0 - \tau_t)}{bc + a} (1 - e^{-(bc+a)x/L}) \quad | \quad (7.6)$$

Since τ_o and τ_t are constant, the amount of sand dropping down G will increase downstream in direct proportion to $(1 - e^{-\lambda x})$. Here, λ is in inverse proportion to L, and L is greater, the faster the wind velocity. Therefore, the faster the wind velocity, the smaller will be λ , and the greater will be the accelerating distance.

Experiments concerning the accelerated flying sand flow were performed in the wind tunnel for the purpose of confirming the above theories. The sand used in the experiments was collected from the beach at Kōnuma in Kanagawa prefecture. Numerous grains of sand were measured with microscopes, and their grain diameter distribution $\phi(d)$ was as shown in Figure 4.

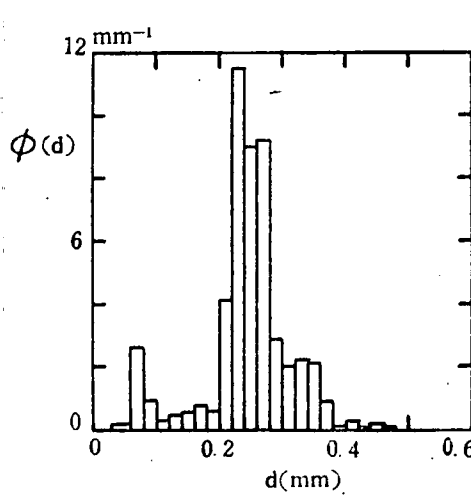


Figure 4. Grain diameter distribution of sand tested.

The average grain diameter was 0.248 mm, and the density was 2.48 g/cm³. This sand was spread over the floor of the wind tunnel with a thickness of about 5 cm, and its upper surface was flattened. Cylinders with an inner diameter of 4 mm were embedded in vertical positions in the sand, so that their upper surface would coincide exactly with the sand surface. These cylinders were installed at intervals of 15 cm and the wind was blown in to make the sand drop into the

cylinders and collect there. Therefore, it is possible to determine the amount of sand dropping down at each point G from the amount in the cylinders and the experiment time. However, the amount dropping down which is found in this manner is not a precise value, as is described below, but is rather an approximate value. Since the sand is removed when the wind blows, there is a drop of the sand surface particularly on the windward side, so that only the cylinders will be protruding above the sand surface. This makes it impossible to make accurate measurements of the amount of sand dropping down, and necessarily the experiment time must be shortened. Since

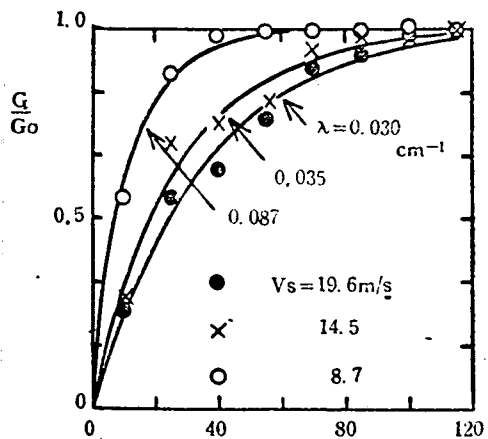


Figure 5. Amounts of sand dropping down in accelerated flow.

the dropping angle of the grains of sand is extremely close to horizontal, it was necessary to place the cylinders accurately with their surfaces in a horizontal position. For these reasons, the accuracy of the experiments was quite low. The experimental results are shown in Figure 5. The V_s in this figure is the wind velocity measured by placing a Pitot tube 30 cm above the sand surface. G_o represents the saturation value of G . The solid lines are the theoretical values $1-e^{-\lambda x}$; the

individual values of λ are written in the figure. The theory of accelerated flying sand flow was proved qualitatively by these experimental results, and the value of λ also decreased with an increase in wind velocity, as one would expect from theory. It was learned clearly from these experiments that the acceleration distance until the flying sand reaches a state of saturation is about 2 m at the most, even when the wind is quite strong. Consequently, in extensive outdoor sandy plains the flying sand flow is in a state of saturation almost everywhere.

8. INTERACTION BETWEEN FLYING SAND AND WIND

/101

It is possible to take photographs of flying sand inside a wind tunnel, by shining bright rays of light from the side and maintaining a constant exposure time. When this is done, the path of the grains of sand shows up in the photographs, and it is possible to determine the speed of the grains of sand in the horizontal direction from the length. It is also possible to use a small Pitot tube under the same conditions to measure the wind velocity inside the layer of flying sand. When the wind velocity at a definite altitude and the mean speed of the grains of sand are compared in this manner, the

latter is always found to be smaller. To mention an example, when the wind velocity at a point with an altitude of 10 cm was 8.5 m/s, the mean speed of the grains of sand at the same point was about 3 m/s.

Consequently, since the momentum of the wind is taken away by the grains of sand within the flying sand layer, it is assumed that the wind velocity will decline. In cases when there is no flying sand, the relationship between the wind velocity and the height follows a logarithmic law, as mentioned above in section 3. However, in cases when there is flying sand there must inevitably be deviations from this law in the flying sand layer. However, since the thickness of the flying sand layer is extremely small, at an altitude of several 10 cm above the sand surface it will be possible to ignore the effects of the flying sand, and the logarithmic law will probably still apply here.

On the other hand, in Equation (7.6) from the previous section, where $x \rightarrow \infty$ the following will apply:

$$G \rightarrow G_0 = b(\tau_0 - \tau_t)/(bc + a)$$

G_0 is the saturation value of G . If we use (7.2) and (7.3), the following will apply in a saturated flying sand:

$$\tau_s = bc(\tau_0 - \tau_t)/(bc + a)$$

Consequently, we will obtain:

$$\tau_w = \tau_0 - bc(\tau_0 - \tau_t)/(bc + a)$$

In actual fact there is an extremely small number of grains of sand which settle down immediately on the sand surface upon collision. Therefore, if we set $a = 0$ in the above equation, we obtain:

$$\tau_w = \tau_t \quad (8.1)$$

This means that at the state of saturation the friction stress of the wind τ_w operating on the sand surface is unrelated to the wind velocity and is always equal to the value of the limiting state. If the wind velocity in the part extremely close to the sand surface is expressed as V_o , τ_w will naturally be in direct proportion to ρV_o^2 in accordance with the concept of dimension. Consequently, (8.1) indicates that the wind velocity directly above the sand surface at the state of saturation is maintained constant, regardless of the wind velocity at a high altitude outside the flying sand layer. From this also it is assumed that the wind velocity inside the flying sand layer will decline in comparison with the case when there is no flying sand.

The wind velocity distribution inside the flying sand layer was measured in the wind tunnel using a multitude type Pitot tube with an inner diameter of 0.6 mm. The sand tested and the experimental conditions were the same as those mentioned above in section 7. The Pitot tube was placed at the farthest downstream part of the wind tunnel (the length of the measuring part of the wind tunnel is 150 cm). As is clear from the experimental results in Figure 5, one can assume that the flying sand has more or less reached saturation at this point.

In experiments of this type, there is the possibility that the grains of sand may fly into the static air inside the Pitot tube, and in this case — in addition to the pressure of the wind itself — the pressure due to the change of momentum of the grains of sand will be added to the Pitot pressure. As for the speed reduction of the grains of sand, it was ignored, since most of it was assumed to be caused by mechanical losses due to collision with the Pitot tube walls. In actual fact, most of the grains of sand entering the Pitot tube stopped several millimeters from the tube entrance, and only rarely did any of them go further inside the tube. Since the Pitot tube is frequently clogged by these grains of sand, the experiments were difficult.

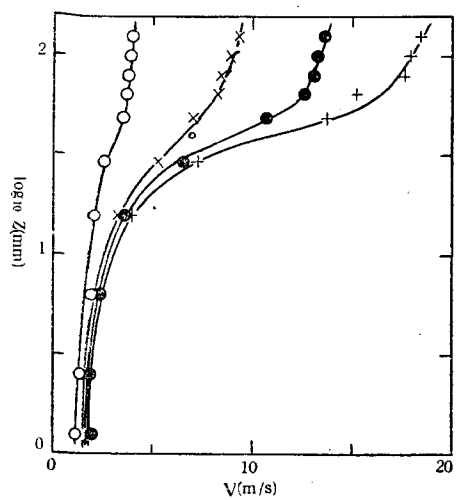


Figure 6. Wind velocity distribution in the vicinity of the sand surface (flying sand is present)

Figure 6 shows some of the experimental results seeking the relationship between the wind velocity inside the flying sand layer and the altitude. A comparison of this figure with Figure 2, which shows the state when there is no flying sand, reveals clearly how the wind velocity declines due to the flying sand. Figure 7 shows the relationship between V_s , the wind velocity at a height 30 cm above the sand surface, and the wind velocity at a definite height inside the flying sand layer.

The experimental values are for

cases when there is flying sand and for cases when there is none (when the sand surface has been moistened). Since there is a high altitude in V_s , it is naturally assumed that it is not influenced by flying sand. The wind velocity at heights of 3 cm and 0.25 cm has a proportional relationship to V_s when there is no flying sand. This is a natural consequence of Prandtl's logarithmic law (3.1). In cases when there is flying sand, when V_s reaches a certain value, the wind velocity at this altitude departs from a straight line and bends over to the side. This indicates that the momentum possessed by the wind is taken away because of the grains of sand. Particularly at an altitude of 0.25 cm, the wind velocity is maintained almost constant with the range where $V_s > 5$ m/s. Since the value of V_s was 4.8 m/s when the grains of sand began to move, near the sand surface the wind velocity will be maintained almost constant at a state above the limiting state. Thus, (8.1) has been proved experimentally. At an altitude of 12.6 cm, even though there may be flying sand, the wind velocity is more or less directly proportional to V_s . Consequently, in the range where $V_s < 20$ m/s, the effect of the flying sand does not extend as far as this altitude. It is clear from this that the thickness of the flying sand layer is extremely small.

/102

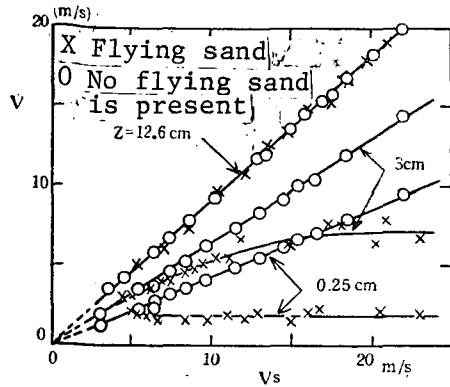


Figure 7. Relationships of wind velocity inside and outside the flying sand layer.

linear relationship between the wind velocity V and $\log z$. The V_τ sought in this manner is in direct proportion to the wind velocity at a definite height (outside the flying sand layer) determined by (3.1). Figure 8 shows the experimental results for the relationship between V_τ and the wind velocity V_s at an altitude of 30 cm. From these experiments, V_τ is expressed as:

$$V_\tau = 0.0488 V_s \quad (8.2)$$

V_τ is very frequently required in various experiments. However, since it is much too complicated to seek V_τ from the wind velocity distribution in every experiment, in most cases we measured only V_s and then calculated V_τ from it, using the experimental Equation (8.2).

The item marked $V_{\tau t}$ in Figure 8 is the limiting friction velocity at the state when the grains of sand are beginning to move. In these wind tunnel experiments, the values were:

$$V_{\tau t} = 23.4 \text{ cm/s},$$

$$V_{st} = 4.8 \text{ m/s}$$

9. QUANTITY OF SAND DROPPING DOWN AND RELATION TO WIND VELOCITY

In this section and all the ensuing sections, we will be discussing cases where the flying sand is in a state of saturation.

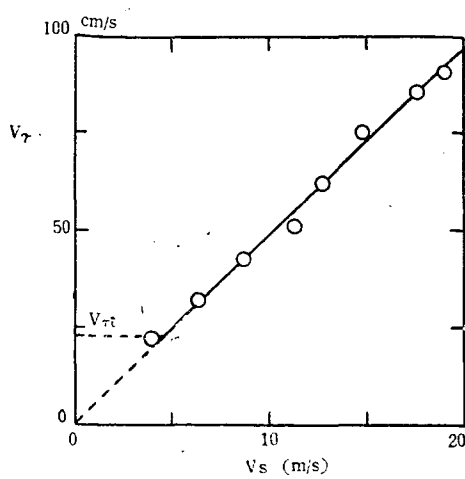


Figure 8. Relationship between friction velocity and V_s (flying sand is present).

At this state, the mass of sand G_0 dropping down onto a unit area of the sand surface per unit time (at the state of saturation, this is identical with the amount leaving the sand surface) is zero below the limiting wind velocity. Beyond this, it increases as the wind velocity increases.

When a cylinder with an inner diameter of 4 mm is stood up vertically at the downstream end of the wind tunnel and its upper surface is brought into alignment with the sand surface, the sand will drop down inside it. Therefore, one can seek G_0 from its weight, the experimental time, and the sectional area of the cylinder. In this case, since the flying sand is in a state of saturation in the measuring section, the height of the sand surface does not vary with the time. Consequently, there are no restrictions on the measuring time, unlike experiments with accelerated flying sand, and it was therefore possible to conduct highly precise experiments.

Figure 9 shows the experimental results, where V_s is the wind velocity at an altitude of 30 cm. It was learned from these results that G_0 and V_s are in a linear relationship. The experimental equation which best matches the experimental values was sought and found to be the following:

$$G_0 = 0.209\rho(V_s - V_{st}) \quad (9.1)$$

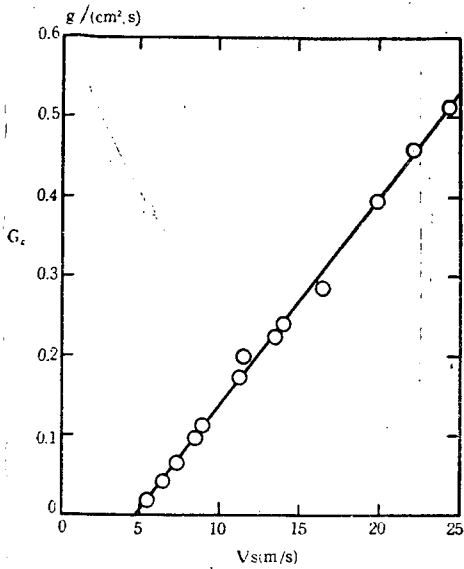


Figure 9. Changes in amount of sand dropping down, G_o , due to wind velocity.

tend to be easily introduced.

Here, V_{st} is the value of V_s at the limiting state, and the value interpolated from the experimental results is

$$V_{st} = 4.8 \text{ m/s} \quad (9.2)$$

This is the most suitable method for determining V_{st} . In the past, attempts were made to determine the point where the grains of sand began to move by mere observations, but it is improbable that accurate values can be obtained, since individual errors of the observer

/103

If we use (8.2) and insert the friction velocity V_τ in place of V_s , (9.1) and (9.2) will be as follows:

$$\begin{aligned} G_o &= 4.28\rho(V_\tau - V_{st}) \\ V_{st} &= 23.4 \text{ cm/s} \end{aligned} \quad (9.3)$$

10. JUMP-OUT SPEED OF THE GRAINS OF SAND, THEIR FLIGHT HEIGHT, FLIGHT DISTANCE, AND TOTAL FLOW RATE

As was stated in (7.2), the friction stress τ_o operating on the sand surface is the sum of τ_s , due to collision of the grains of sand, and τ_w , due to the wind. Since (8.1) also holds at the state of saturation, the following may be assumed

$$\tau_s = \tau_o - \tau_w \quad (10.1)$$

τ_s is produced because the grains of sand collide with the sand surface

and lose their momentum in the x-direction. The following can be set

$$\tau_s = G_o (\overline{u_2 - u_1})$$

The numbers 1 and 2 indicate the values when the grains of sand jump out and when they drop down, respectively, and the horizontal bar indicates the mean value. In cases of inelastic collision, there is generally a proportional relationship between the forces which are perpendicular to the plane and the forces which are parallel. However, in this case also, if we assume the same relationship, we can set the following:

$$G_o \mid (\overline{u_2 - u_1}) \mid = \xi G_o \mid (\overline{w_2 - w_1}) \mid$$

Here, ξ is a proportional constant. On the other hand, since $\overline{w_2 - w_1} = -2\overline{w_1}$ from (6.8), in the final analysis we obtain the following:

$$\tau_s = 2\xi G_o \overline{w_1} \mid \quad (10.2)$$

On account of (10.1) and 10.2), we obtain either

$$\text{or} \quad 2\xi G_o \overline{w_1} = \tau_o - \tau_t, \quad (10.3)$$

$$2\xi G_o \overline{w_1} = \rho(V_\tau^2 - V_{\pi^2}) \mid$$

On the other hand, since (9.3) applies to the relationship between G_o and V_τ , the relationship between $\overline{w_1}$ and V_τ will be as follows:

$$\overline{w_1} = K_1 (V_\tau + V_{\tau t}), \quad K_1: \text{Constant} \quad (10.4)$$

Next, from the standpoint of statistical probability, u_1 and w_1 are independent. If $\overline{w_1^2}$ is assumed to be approximately identical to $\overline{w_1}^2$, it will be possible to determine the relationship between the mean value of the flight distance and the flight height and V_τ in the following pattern, from

(6.9)

$$\left\{ \begin{array}{l} \bar{L} = K_2 \frac{(V_\tau + V_{\tau t})^2}{g}, \\ \bar{h} = K_3 \frac{(V_\tau + V_{\tau t})^2}{g}, \end{array} \right. \quad \begin{array}{l} K_2: \text{ Constant} \\ K_3: \text{ Constant} \end{array} \quad (10.5)$$

If we consider the vertical plane of the unit width at a right angle to the main wind, the quantity of sand moving through this plane per unit time will represent a percentage of the total flow rate of the flying sand at that time. If this quantity is expressed as Q , in terms of averages Q will be expressed approximately by the following equation

$$Q = G_0 \bar{L} \quad (10.6)$$

If we insert (9.3) and (10.5) in this equation, we obtain:

$$Q = K_4 \frac{\rho}{g} (V_\tau - V_{\tau t})(V_\tau + V_{\tau t})^2 \quad (10.7)$$

K_4 : Constant

In the equations above, K_1 , K_2 , K_3 , and K_4 are all dimensionless constants, but they will probably assume somewhat different values due to the mean diameter of the sand grains and the state of the sand surface.

With reference to Q , Bagnold obtained the following [2]:

$$Q = \text{const. } \rho V_\tau^3 / g, \quad V_\tau \geq V_{\tau t}$$

In cases when $V_\tau \gg V_{\tau t}$ — that is, when there is an extremely strong wind — this equation coincides with (10.7), but there is generally no agreement when V_τ assumes its ordinary value. In Bagnold's equation, Q does not become zero even when $V_\tau = V_{\tau t}$. However, in (10.7) these conditions are

satisfied, and (10.7) is more reasonable from this point of view.

Experiments concerning the total flow rate were conducted both in the wind tunnel and outdoors (at the Ikeshinden beach in Shizuoka prefecture in February and March, 1949). The outdoor experiments were carried out on a relatively flat sandy beach where strong seasonal winds blow almost parallel to the sea coast. This is the most suitable place for flying sand experiments. /104 The grain diameter distribution of the sand grains on this beach is shown in Figure 10. The mean grain diameter was 0.307 mm, and the density was 2.50 g/cm^3 .

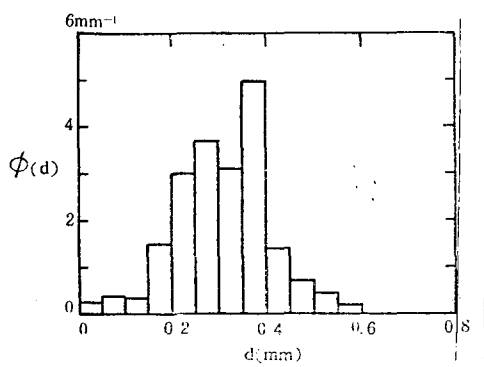


Figure 10. Distribution of sand grain diameter at outdoor experimental site.

The same sand as that described already was used in the wind tunnel experiments. The sand was spread out on the floor of the wind tunnel, and the total weight of the sand was measured in advance. Next, a constant wind was allowed to blow for a certain time, so that some of the sand in the measuring section would be carried away by the wind. After the experiment,

the weight of the sand remaining in the measuring section was measured, and the difference between this and the weight of the sand before the experiment was sought. The result amounts to the quantity of the sand which flowed over the vertical surface downstream of the measuring section of the wind tunnel during the experiment. Thus, it is possible to determine the total flow rate Q from the width of the wind tunnel (5 cm) and the experiment time. As was mentioned before, even when the wind is quite strong the flying sand is in a state of saturation at the furthest downstream part of the measuring section, but when V_s (the wind velocity at an altitude of 30 cm) rose above 20 m/s, the sand surface at the furthest downstream part gradually dropped during the experiment. Consequently, this part had not yet reached a state of saturation, and it was expected that the experimental value of Q would be

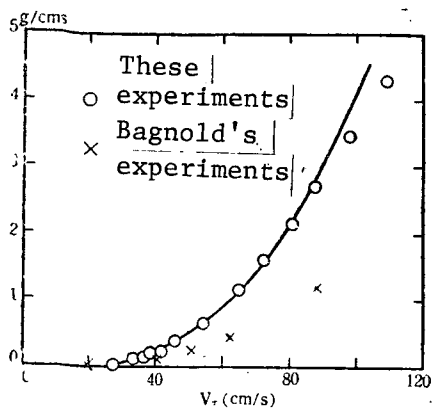


Figure 11. Total flow rate Q (wind tunnel experiments).

the abscissa were sought from the measured values of V_s by using (8.1). The solid line in the figure shows the theoretical value of Q (10.7) when $K_4 = 2.78$ was assumed. When $V_\tau > 90$ cm/s, the experimental values were lower, but this could be attributed to the fact that the measuring section in the wind tunnel had a short length and had not yet reached the state of saturation. Since there was extremely good agreement between theory and experiments in the other regions, one may say that the validity of (10.7) was proved. The experimental values of Bagnold are entered in the figure; these values are much smaller than the experimental values of the writer. The reason for this discrepancy is unclear, but it is assumed that it is probably due to differences in the experimental method (Bagnold adopts a method of supplying the sand artificially from upstream).

In outdoor experiments it is impossible to measure Q by means of the same method used in the wind tunnel; therefore, a method of directly collecting the actual flying sand was adopted. The item requiring the most attention when collecting flying sand is to see that the flow of air and sand will be disturbed as little as possible by the collecting instrument. When the pattern of flow is changed by the collecting instrument, there will be an extreme drop in the capture rate by the collecting instrument. Particularly close attention must be paid to places very close to the sand surface, since the kinetic energy of the sand is small in these places.

lower than the value at the state of saturation. In experiments with such strong winds, it will no doubt be necessary to increase further the length of the measuring section of the wind tunnel.

Figure 11 is a comparison of the results of wind tunnel experiments with reference to Q and the theoretical values. The values of V_τ plotted on

Barkhan type dunes are often formed on the windward sides of obstacles such as houses or woods in deserts, and the same reason explains why the sand does not reach as far as the obstacle. Taking this point into consideration, we prepared a horizontal type sand collector for measuring Q in outdoor experiments. This sand collector is a box 50 cm long, 15 cm wide, and 10 cm deep; the top is open. Two partition boards are located in the lengthwise direction; they divide the interior up into three sections each 5 cm in width. At the rearmost end of the central section, a 200 mesh wire net is installed at an altitude of 10 cm over the top, so that the sand hitting this part will fall into the central part of the box. When this sand collector is buried in the sand so that the upper surface is aligned with the sand surface and so that its length coincides with the direction of the prevailing wind, most of the flying sand will fall down into the box, either directly or after colliding with the wire net. The percentage of sand grains which fly across the wire net and escape may be extremely small in view of the flight distance of the grains of sand, as described below. It is desirable for the sand collector to be as long as possible, but a length of 50 cm was adopted because of the ease of operation. The sections 5 cm wide on both of the sides were provided so that the grains of sand coming in from both sides of the box (those with a velocity v other than zero) would not enter the central part. After sand was collected for a suitable time in this sand collector, the sand accumulated in the central part was weighed. By dividing this by the width at the front (5 cm) and the duration of collection, it is possible to obtain the value of Q for that time. A Biram type anemometer was placed 1.2 m above the sand surface, and the mean value of the wind velocity was measured by it during the entire time of collection. When this is taken as V , we can assume that Prandtl's logarithmic law (3.1) applies to the relationship between V and the V_s (wind velocity at an altitude of 30 cm) used as standard in the wind tunnel experiments. Since the size of the sand grains is almost the same, we can assume that the coarseness k is also constant. Under these assumptions, the following may be assumed

$$V = 1.14 V_s \quad (10.8)$$

In the outdoor experiments, there never was a strong wind within the range of $V > 16$ m/s. The experimental results are shown in Figure 12, where the wind tunnel experimental values and the theoretical values are added in values converted into V . The agreement between the three was good in most cases. Since these are difficult experiments carried out in the midst of strong winds and intense sandstorms, it would be impossible to anticipate any results better than these.

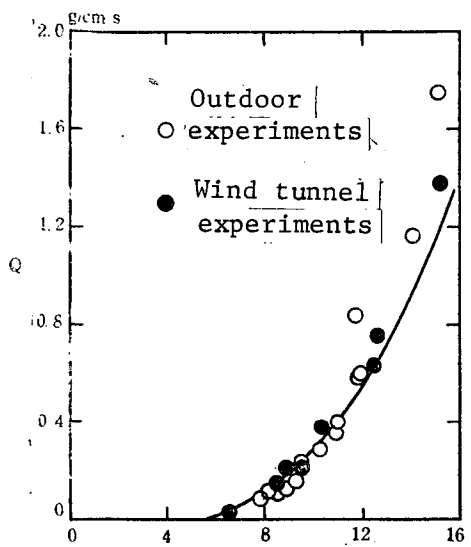


Figure 12. Total flow rate Q
(outdoor experiments)

of probable density of the upwards jumping-out speed w_1 in saturated flying sand flow. Let us assume that this probable density is $\phi(w_1)$. It will be constant at the state of saturation, and ϕ will not be related to the time. Therefore, the following diffusion equation is used as the differential equation to find ϕ

$$-m_1 \frac{d\phi}{dw_1} + \frac{1}{2} m_2 \frac{d^2\phi}{dw_1^2} = 0 \quad (11.1)$$

As boundary conditions, it is valid to assume that $d\phi/dw_1 = \phi = 0$ when $w_1 = \infty$. Under these conditions, the following solution will be valid for (11.1):

$$\phi(w_1) \propto e^{-\mu w_1}, \quad \mu: \text{Constant} \quad (11.2)$$

11. DENSITY DISTRIBUTION OF SAND GRAINS INSIDE THE FLYING SAND LAYER

In the previous section the discussion pertained solely to the average quantities of the flying sand. Next, let us proceed with a statistical treatment, considering the flying sand as the motion of numerous grains of sand.

For this purpose, it is first of all necessary to determine the degree

However, with respect to m_1 and m_2 in (11.1), based on the present state of our knowledge, we are unable to say anything decisive, and in this sense it would be difficult to assume that the solution in (11.2) has any important theoretical foundation. Let us merely adopt the relatively simple solution in (11.2) as a hypothesis, and determine the validity of this hypothesis by comparing the theoretical results with the experiments.

Since the relationship $h = w_1^2/2g$ given in (6.9) applies between w_1 and the flight height h (the maximum altitude which the grains of sand can reach), the following must apply if $f(h)$ is the probability function of h :

$$f(h)dh = \phi(w_1)dw_1$$

Consequently, in view of (11.2), $f(h)$ will assume the following form

$$f(h) = \frac{1}{\sqrt{2h_0}} \frac{1}{\sqrt{h}} e^{-\sqrt{2h/h_0}} \quad (11.3)$$

Here, h_0 is the mean value of h , amounting to the following:

$$\int_0^\infty h f(h) dh = h_0$$

Next, let us use Ψ as the mass of the sand contained in a unit volume in the flying sand layer. Ψ is a function of the height z , and also probably fluctuates with time. Here, however, we shall consider its temporal mean value. The grains of sand jumping up from the sand surface have various flight heights h , following the distribution shown in (11.3). Those among them having a flight height between h and $h + dh$ shall be called the sand grains belonging to the aggregate S_h . If we consider only the grains belonging to S_h , we can use $\Psi_h dh$ as the density of these grains at height z . If we consider a horizontal plane where $z < h$, the flow rate of the grains in aggregate S_h which rise or fall passing through a unit area on this surface

must in all cases be equal to the mass of the grains of S_h which jump out from a unit area of the sand surface. That is, it is identical to $G_0 f(h)dh$. On the other hand, according to (6.7) the absolute values of the rising and falling speeds of grains of sand at height z are identical to each other. Therefore, from the point of view of averages, half of the sand grains comprising the density $\Psi_h(z)dh$ will be moving upwards, and half of them will be moving downwards. The following equation results from the above considerations

$$\Psi_h dh w_h = 2G_0 f(h)dh \quad (11.4)$$

Here, w_h is the rising speed of the grains of sand belonging to S_h . It is expressed in the following manner in view of (6.7) and (6.9).

$$w_h(z) = \sqrt{2g(h-z)} \quad (11.5)$$

The following relationship must hold between Ψ_h and the actual density Ψ

$$\Psi(z) = \int_z^\infty \Psi_h dh \quad (11.6)$$

Here the lower integration limit was set at z , because grains of sand belonging to the aggregate S_h , where $h < z$, do not reach a height z and play no part at all in the density at that point.

When (11.3), (11.4) and (11.5) are substituted in (11.6), the following is assumed

$$\Psi(z) = \frac{G_0}{\sqrt{gh_0}} \int_z^\infty \frac{1}{\sqrt{h(h-z)}} e^{-\sqrt{2h/h_0}} dh \quad (11.7)$$

If it is assumed that $h = z \cosh^2 \theta$, the following holds

$$\Psi(z) = \frac{2G_0}{\sqrt{gh_0}} \int_0^\infty e^{-\sqrt{2z/h_0} \cosh \theta} d\theta$$

On the other hand, according to the integral representation of Bessel functions [13], the Bessel function $K_\nu(x)$ will be expressed as follows:

$$K_\nu(x) = \int_0^\infty e^{-x \cosh \theta} \cosh \nu \theta \cdot d\theta \quad (11.8)$$

Consequently, in the final analysis we obtain the following:

$$\psi(z) = \frac{2G_0}{\sqrt{gh_0}} K_0(\sqrt{2z/h_0}) \quad (11.9)$$

This equation is an equation expressing the density distribution of the grains of sand.

In (11.9), $K_0(x)$ becomes infinitely great at $x \rightarrow 0$. Therefore, if we were to interpret this at face value, it would appear that the sand grain density ψ would become infinitely great on the surface of the sand. This would appear to be a physical impossibility. However, this occurred because the sizes of the sand grains were omitted. Since it would be meaningless in this argument to discuss sizes smaller than the sizes of the sand grains, there is no physical contradiction in assuming $\psi \rightarrow \infty$ at $z \rightarrow 0$. The same thing arises in Prandtl's logarithmic law (3.1) concerning the wind velocity distribution.

Next, calculating by gradual development, we obtain the following at $z \rightarrow \infty$:

$$\psi \frac{d(\log \psi)}{dz} \rightarrow -\frac{1}{\sqrt{2h_0z}}$$



On the other hand, the following is obtained by means of Exner's diffusion theory:

$$\psi = Ae^{-Bz} \quad (A, B: \text{constants})$$

In this case, $d(\log \psi)/dz$ becomes a constant. Consequently, even when z is

large, there are differences between this theory and the Exner theory. However, when the value of x is small, $\log K_0(x)$ increases rapidly, while it changes only slowly where the value of x is great. Consequently, if one were to measure only Ψ at high altitudes, this would not bring about a very clear differentiation between this theory and the Exner theory.

Experiments to determine the distribution of the sand grain density Ψ were carried out in the wind tunnel using photoelectric tubes. Since the grains of sand are minute particles, they behave in the same manner as absorbent substances with respect to light in the range where the spatial density has not yet become too great, and it is assumed that the degree of absorption is in direct proportion to Ψ , the spatial density of the grains of sand. If we assume that the light intensity I decreases by dI while moving forward over a distance dx , the following equation will apply

$$-(dI/dx) = (C + D\Psi)I \quad (11.10)$$

Here, C is the absorption coefficient of the spatial substance, and D is a constant.

If we assume that $I = I_0$ when $\Psi = 0$ and $x = L$, then the solution of the above equation will be either

$$I = I_0 e^{-DL\Psi}$$

or

$$\log(I/I_0) = -DL\Psi \quad (11.11)$$

Consequently, when L is known, one can determine D by measuring I_0 , I and Ψ . Once D has been found, when Ψ is unknown, it can be discovered by measuring I_0 and I .

The following experiments were performed to determine D . Parallel light rays were shined into a glass container 3.8 cm wide containing 200 cc of glycerine. This passed through a narrow slit on the opposite side of the

container, and was received by the photoelectric tube. A galvanometer was placed in the photoelectric tube circuit, and the photoelectric current was measured. The quantity $A_o - A_s$, the difference between the photoelectric current when the light was shined (A_o) and that when the light was cut off (A_s), is in direct proportion to I_o . Next, sand with mass M was mixed in the glycerine and stirred well. When the sand was uniformly diffused in the glycerine, the same measurements as above were performed. If the photoelectric current obtained at this time is A , then $A - A_s$ will be in direct proportion to the I in (11.11). Consequently, the following equation will hold

$$I/I_o = (A - A_s)/(A_o - A_s)$$

Since Ψ at this time is $(M/200)\text{g/cm}^3$, if the same experiments are continued, changing the value of M , it will be possible to determine the relationship between I/I_o and Ψ . The experimental results are shown in Figure 13. As was anticipated, it was found that $\log(I/I_o)$ is in direct proportion to Ψ . From these results, it was possible to determine the value of D as $D = 37.5 \text{ cm}^2/\text{g}$.

/107

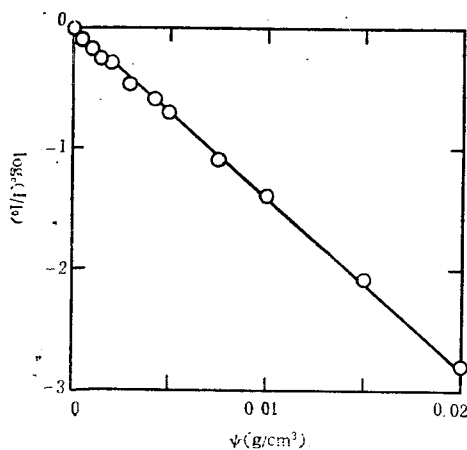


Figure 13. Reduction of luminous intensity by grains of sand.

Since both sides of the wind tunnel used are made of glass plate, it was possible to apply the above-mentioned equipment without changing to flying sand inside the wind tunnel. In these experiments, the photoelectric tube and the slit (height 1.4 mm) were gradually moved away from the sand surface, and I_o and I were measured at each altitude. $\Psi(z)$ was sought by means of (11.11) from the known value of D and from

the width of the wind tunnel (5 cm). Some of the experimental results are shown in Figure 14, which shows the relationship between $\log \Psi$ and the

height z . The results are given for three wind velocities. The solid lines in the graph are the values of $\log K_0 (\sqrt{2z/h_0}) + \text{const.}$ at the time when the value of h_0 was suitably established, so that the various experimental locations would be well plotted. The various values of h_0 are given in the graph.

The most obvious conclusion from these results is the fact that the value of $\log \Psi$ increases suddenly in the vicinity of the sand surface. Consequently, it is found that Exner's results are clearly incorrect. It is also obvious from the graph that Ψ declines rapidly together with z , and

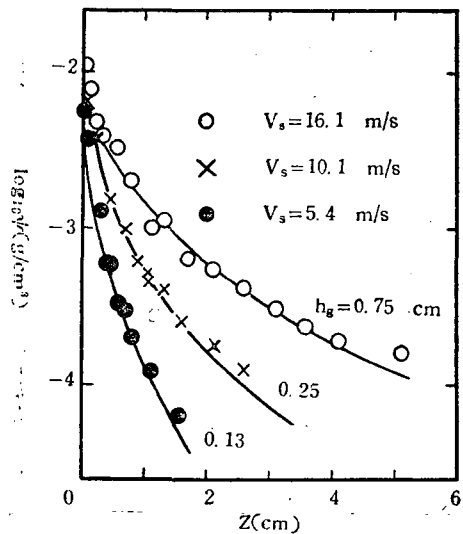


Figure 14. Sand grain density distribution.

that h_0 (the mean value of h) is less than 1 cm even when the wind is quite strong. It is clear, therefore, that most of the flying sand is in an extremely low layer. A comparison of the experimental results and the theory reveals that in Figure 14 the state at which Ψ decreases together with z coincides almost perfectly with the theory. The actual value of Ψ can be calculated by (11.9) if h_0 and G_0 are known. Using the value obtained

from (9.1) or (9.3) for G_0 , one can calculate Ψ at the height of $z - 1$ cm. When the values are compared with the experimental values, the results are as shown in Table 1. There is a generally satisfactory agreement between both, with the exception of cases where $V_s = 5.4$ m/s (a wind velocity slightly higher than the limiting state).

The correctness of theoretical Equation (11.9) was proved by the experimental results given above. In the final analysis, this shows that the first hypothesis concerning the distribution of w_1 (11.2) is correct.

TABLE 1

V_s (m/s)		16.1	13.2	11.2	10.1	7.9	5.4
$\Psi \times 10^3$ (g/cm ³)	Theoretical values	3.3	2.0	0.98	0.68	0.26	0.05
	Experimental values	1.8	1.4	1.00	0.63	0.40	0.18

As is clear from Table 1, the density of sand grains at a height of 1 cm above the sand surface is about 10^{-3} to 10^{-4} g/cm³. The magnitude is approximately the same as the density of the air. Since the mass of one grain of sand is about 2×10^{-5} g, it is concluded that about 30 to 100 grains of sand are present in a volume of 1 cc in this vicinity.

Next, it is possible to seek the value of h_o at each wind velocity by means of these experiments. Figure 15 shows the relationship between $\log h_o$ and $\log(V_\tau + V_{\tau t})$. Since the h in (10.5) has the same meaning as h_o , the following relationship ought to hold between h_o and V_τ :

$$h_o = K_3(V_\tau + V_{\tau t})^2/g$$

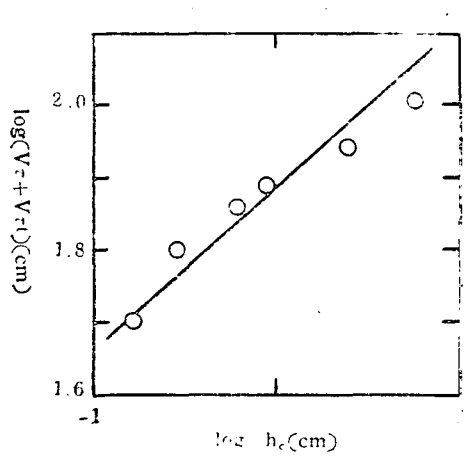


Figure 15. Relationship between mean values of flight height and wind velocity.

In Figure 15, the solid line connecting the experimental values of $\log h_o$ and $\log(V_\tau + V_{\tau t})$ has a gradient of 2.2. This shows that the above relationship is more or less satisfied.

/108

12. FLYING SAND RATE DISTRIBUTION IN TERMS OF HEIGHT

The percentage of the flying sand rate at a definite height z , $q(z)$, is the product of the sand grain density at that point, $\Psi(z)$, and the

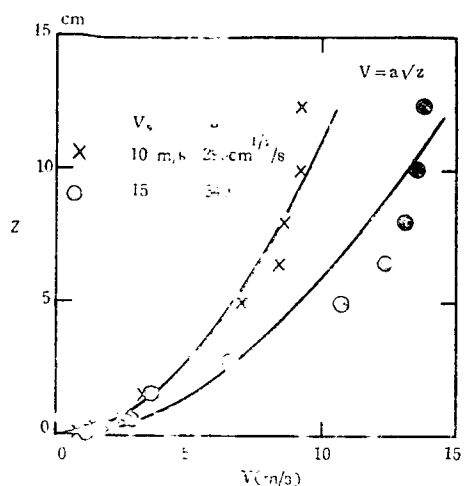


Figure 16. Wind velocity distribution in flying sand layer.

mean speed of the sand grains in the x direction, \bar{u} .

Now let us return to the previous point and consider the grains of sand belonging to aggregate S_h (those with a flight height between h and $h + dh$). If the flow rate of the sand grains at this height z is $q_h dh$, and if the mean velocity in the x direction is \bar{u}_h , then

$$q_h dh = \bar{u}_h \rho S_h dh$$

(12.1)



Since the wind velocity inside the flying sand layer is faster the higher the altitude, \bar{u}_h will become faster the greater is h . Consequently, when dealing with the flow rate distribution, it is necessary to take into consideration changes in the wind velocity due to the height. However, since exact calculations are impossible, let us proceed with calculations by means of the following two approximations:

- 1) The wind velocity V inside the flying sand layer is expressed by the following

$$V = a\sqrt{z}$$

(12.2)

- 2) The grains of sand belonging to S_h are subjected to a constant wind velocity V_h at all times during their motion. The wind velocity at a height of $z = 0.75h$ is taken as V_h

$$V_h = a\sqrt{0.75h}$$

(12.3)

Figure 16 gives the experimental results for the wind velocity distribution in the vicinity of the sand surface in cases when there is flying sand. The solid lines in the graph are the calculated values of $V = a \sqrt{z}$ when suitable values were supplied for a . From these experimental results one may conclude that the first hypothesis is valid in an approximate manner. The second hypothesis was adopted entirely for the purpose of simplifying the calculations, and the validity of the number 0.75 must be determined according to the experimental results.

Since the speed in the x-direction of grains of sand moving under the influence of a definite wind velocity has already been found in (6.5), if V_h is substituted for the V in this equation, and if w_1 is expressed by means of h in accordance with (6.9), the following equation is obtained.

$$u_x = u_1 + \sqrt{\frac{2}{g}} \beta (V_h - w_1) \sqrt{h} \left(1 + \sqrt{1 - \frac{z}{h}} \right) \quad (12.4)$$

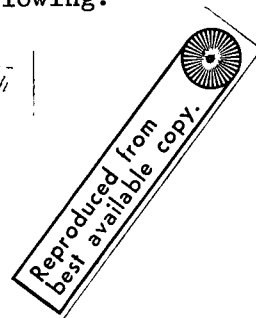
Next, when this equation is averaged for a large number, the falling time and the rising time cancel each other, and the right-hand term containing cross terms disappear. Since u_1 and w_1 are assumed to be independent from the standpoint of probability, the mean value of w_1 will cease being related to h . Consequently, using (12.3), we obtain the following:

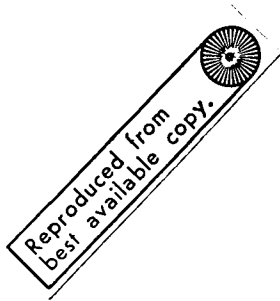
$$\bar{u}_x = \bar{u}_1 + \sqrt{\frac{2}{g}} \beta (0.75 \bar{h} - \bar{u}_1) \sqrt{\bar{h}} \quad (12.5)$$

The flow rate $q(z)$ is expressed as follows

$$q(z) = \int_0^z q_1 dh + \int_0^z \Psi_h \bar{u}_x dh \quad (12.6)$$

Since Ψ_h has already been obtained in the preceding section, and since we already know \bar{u}_x from (12.5), it is possible to calculate (12.6). The results are expressed as in the following by three integrations





$$\begin{aligned}
 q(z) &= \frac{G_0}{\sqrt{g h_0}} \left[\bar{u}_1 I_1 - \sqrt{\frac{2}{g}} \beta \bar{u}_1 I_2 + \sqrt{\frac{1.5}{g}} a \beta I_3 \right], \\
 I_1 &= \int_z^\infty \frac{1}{\sqrt{h(h-z)}} e^{-\sqrt{2h/h_0}} dh, \\
 I_2 &= \int_z^\infty \frac{1}{\sqrt{h-z}} e^{-\sqrt{2h/h_0}} dh, \\
 I_3 &= \int_z^h \sqrt{\frac{h}{h-z}} e^{-\sqrt{2h/h_0}} dh.
 \end{aligned}$$

All of these integrations are expressed using Bessel functions by substitution of $h - z \cosh^2 \theta$. That is,

$$\begin{aligned}
 I_1 &= K_0\left(\sqrt{2\frac{z}{h_0}}\right), & I_2 &= 2\sqrt{z} K_1\left(\sqrt{2\frac{z}{h_0}}\right), \\
 I_3 &= \left[K_0\left(\sqrt{2\frac{z}{h_0}}\right) + K_2\left(\sqrt{2\frac{z}{h_0}}\right) \right].
 \end{aligned}$$

Consequently, $q(z)$ will assume the following final form

$$\begin{aligned}
 q(z) &= \frac{G_0}{\sqrt{g h_0}} \left[\lambda \left\{ 2\sqrt{2} K_0(\xi) - 2\sqrt{2} \beta \sqrt{\frac{h_0}{g}} \xi K_1(\xi) \right\} \right. \\
 &\quad \left. + \frac{1}{2} a \beta \sqrt{0.75 h_0} \xi^2 \left\{ K_1(\xi) + K_3(\xi) \right\} \right]
 \end{aligned}$$

(12.7)

$$\xi = \sqrt{2z/h_0}, \quad \lambda = \bar{u}_1 / \sqrt{2gh_0}.$$

Even though various hypotheses were used to simplify the calculations, the results in (12.7) are quite complex. Nevertheless, if it is possible to find a and λ , they can be used to find the distribution of the flow rate. We already described a . λ is the ratio of \bar{u}_1 and $\sqrt{2gh_0}$, and the latter is also approximately identical to \bar{w}_1 . Consequently, many measurements can be taken of the angles at which the grains of sand jump out, and the approximate value of λ can be determined from this. The value sought from photographs of the flying sand inside the wind tunnel was $\lambda \approx 2$.

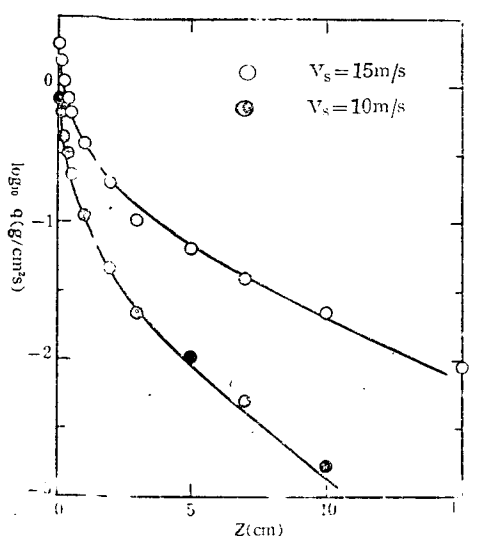


Figure 17. Distribution of flying sand in terms of height (wind tunnel experiments).

The $q(z)$ given by (12.7) has more or less the same form as $\Psi(z)$; where the value of z is small, $q(z)$ increases rapidly. At $z \rightarrow 0$, we find that $q \rightarrow \infty$. However, as was explained for Ψ , this fact does not necessarily involve any physical contradiction. Where there is a large value of z , it is found that $q \sim \xi^{3/2} e^{-\xi}$.

In order to establish the distribution of the flying sand by experiments, it is necessary to capture and collect the flying sand at a definite altitude by some method.

As was already mentioned concerning measurements of the total flow rate, the sand collector must be one which disturbs the flow of the wind and sand as little as possible. When measuring the total flow rate, this was attained by using a horizontal type sand collector, but a Pitot tube type sand collector was used to measure the flying sand distribution. The sand collector is arranged with rectangular sand collecting holes directly facing the wind. The sand which flies into these holes moves down along the tube and falls into the container below. In this case, the air flow is naturally disturbed by the sand collector, but the range disturbed is in direct proportion to the size of the sand collector. If this range is too broad, the sand will be unable to reach the sand collector, but if the section with the disturbed air flow is restricted, the grains of sand will fall into the sand-collecting holes of their own inertia. Therefore, in order to obtain a capture rate close to 1, the size of the section with the disturbed air flow must be small enough in comparison with the flight distance of the grains of sand. In consideration of this, the sand collectors used were made as small as possible. In wind tunnel experiments, collectors with sand collecting holes 2 mm high and 7 mm wide were gradually moved upwards

or downwards to measure the distribution of the flying sand. Since this procedure was not possible in outdoor experiments, nine sand collectors were set up to a height of 30 cm from the sand surface, and measurements were made simultaneously. Since the amount of flying sand is smaller, the higher the altitude, if the sand-collecting holes are given a constant area, the amount of sand collected in a definite time will vary greatly depending on the altitude, and there will be inaccuracies when measuring the weight. Therefore, the sand collectors at higher altitudes were given larger sand collecting holes. Since the grains of sand flying at higher altitudes have a greater kinetic energy, it does not matter (from the viewpoint of the capture rate) if the sand collectors are somewhat large.

Some of the results of the wind tunnel experiments are shown in Figure 17, which gives the results for two values of $V_s = 15$ and 10 m/s. The solid lines indicate the theoretical values when it was assumed that $\lambda = 2$ in (12.7), and the values corresponding to each of the states were inserted into a. It was found as a result that there was good agreement between the

/110

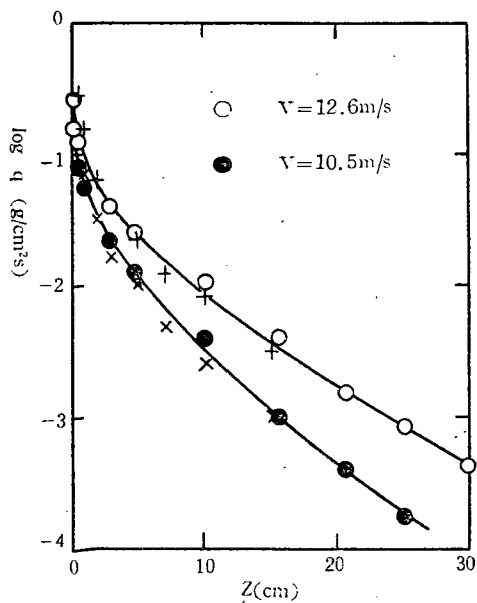


Figure 18. Distribution of flying sand in terms of height (outdoor experiments).

theoretical values and the experimental values. Figure 18 shows the results of the outdoor experiments, where wind velocity V is the mean value at an altitude of 1.2 m. Since the relationship between the standard wind velocity V in outdoor experiments and that in the wind tunnel experiments, V_s , has already been given by (10.8), it is possible to carry out wind tunnel experiments corresponding to the conditions in outdoor experiments. The values of the wind tunnel experiments which are given in the graph in Figure 18 correspond to each of the outdoor experiments in this sense.

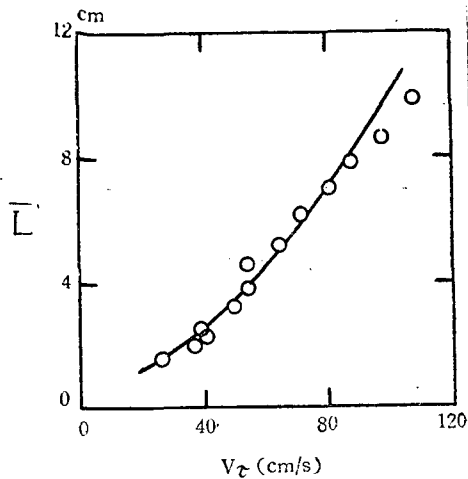


Figure 19. Mean values of flight distance.

flying sand distribution corresponds so well indicates the correctness of the assumptions of Bagnold and the author, who hold that the effects of wind turbulence on flying sand may be ignored.

As is clear from this graph, there is good agreement between the outdoor experiments and the wind tunnel experiments as far as the flow rate distribution is concerned. Natural wind has a much greater intensity and scope of turbulence than artificial air currents inside a wind tunnel, and the properties of both are entirely different as far as the turbulence of the air flow is concerned.

Nevertheless, the fact that the

13. FLIGHT DISTANCE OF FLYING SAND AND ITS DISTRIBUTION

Let us use L to represent the distance traversed in one jump by grains of sand in motion, and \bar{L} — to represent their mean value. In accordance with (10.6), the value will be

$$\bar{L} = Q/G_0$$

Since Q and G_0 can each be measured directly by wind tunnel experiments, it is possible to find \bar{L} . Figure 19 gives the results when the calculated value of G_0 from experimental Equation (9.3) is used. \bar{L} is calculated back from the experimental value of Q in Figure 11, and the relationship with V_τ is sought. On the other hand, \bar{L} is given theoretically by (10.5). The solid line in Figure 10 represents the calculated values when it is assumed in (10.5) that

$$K_2 = 0.649$$

Naturally, there is good agreement between theory and experiments. It was also established from these results that, even when the wind is quite strong, the mean value of the flight distance of sand grains is at the most about 10 cm.

Next, it is assumed that the flight distances L of individual grains of sand are not identical, but have a certain distribution. This distribution function is $g(\xi)$. Let us take a point of origin on the sand surface and plot the direction of the prevailing wind on the x -axis. Let us furthermore assume that, although sand does jump out from the range where $x < 0$, sand which drops down in the range where $x > 0$ is only absorbed and no sand jumps out. If $F(x)$ is the amount of sand dropping down per unit time onto a unit area where $x > 0$, this is the total of the sand (which jumped out from the range where $x < 0$) which happened to drop down into exactly this section on account of the flight distance. Therefore, it can be written as

$$F(x) = G_0 \int_{-\infty}^0 g(x - \xi) d\xi \quad (13.1)$$

where g is the distribution function. If we take into consideration the fact that

$$\int_0^{\infty} g(\xi) d\xi = 1$$

we obtain the following:

$$F(x) = G_0 \left[1 - \int_0^x g(t) dt \right] \quad (13.2) \quad \underline{/111}$$

Consequently, we obtain:

$$g(x) = -(dF/dx)/G_0 \quad (13.3)$$

Therefore, if we find $F(x)$, it will be possible to find g , the distribution function of the flight distance.

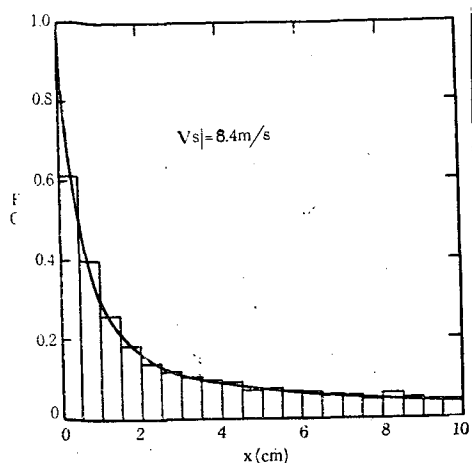


Figure 20. Distribution of $F(x)$.

Experiments to find $F(x)$ were carried out in wind tunnels in the following manner. A box with an open top was placed in a horizontal position at the furthest downstream part of the measuring section of the wind tunnel, and its upper surface was aligned with the height of the sand surface. This box has a length of 10 cm, and it is partitioned into 20 divisions at intervals of 0.5 cm by means of vertical partition plates standing at right angles to the prevailing wind. These partition plates are made so that their upper surfaces also will be aligned with the sand surface or the upper surface of the box. When this box was installed and the wind began to blow, the sand would fall into the box, and sand was accumulated in each of the divisions. After a suitable time had gone by, the box was taken out, and the sand in each of the compartments was weighed. When this weight was divided by the area and the time, it was possible to obtain a stage distribution curve which clearly corresponds to $F(x)$. Since $F(0) = G_0$ from (13.2), it is possible to connect this stage-type distribution with a smooth curve and to determine G_0 at each time from the point where this curve intersects the point of origin. Typical examples of the experimental results are shown in Figure 20. If the smooth curve in this graph is subjected to first-order differentiation, it will be possible to use (13.3) to obtain the flight distance distribution g . The results of this are as shown in Figure 21.

In most cases the flight path of the grains of sand is extremely close to the horizontal in the vicinity of the drop-down point. Therefore, in order to perform the above-mentioned experiments accurately, the box must be placed in a perfectly horizontal position, and the height of all of the partition plates must be aligned with the sand surface. However, under

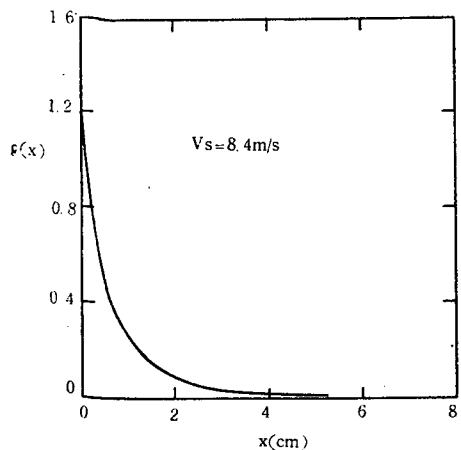


Figure 21. Flight distance distribution.

conditions when the wind was blowing, it was not possible to maintain the height of the sand surface exactly constant, and therefore it was impossible to carry out these experiments accurately. The fact that there are ups and downs along the stage distribution in Figure 20 indicates that there were slight unevennesses in the partition plates. When seeking the flight distance distribution g , a differential operation is performed once, and therefore high accuracy can hardly be anticipated. One may say that the general trend is for the vast majority of grains to have a small flight distance. The same trend applies even to cases when there is a great wind velocity, the only difference being that the mean value moves towards a greater distance. The flight distance L is related to both u_1 and w_1 , which are given by (6.9). However, in general those with a greater value of w_1 also have a larger L . Consequently, the fact that the flight distance distribution g has a larger value, the smaller is L , signifies that the distribution of w_1 is greater when w_1 is smaller. This shows that the hypothetical distribution of w_1 given above (11.2) is valid.

In connection with the flight distance distribution, let us add the following. First, as already mentioned,

$$G_0 = F(0)$$

Therefore, an accurate value cannot be obtained in measuring the amount of sand dropping down, G_0 , when using a sand collector with spaces of a certain size. Consequently, the values of G_0 found in section 9 are also approximate values. Bagnold provided small crevices in the sand surface and stipulated that the grains of sand falling into them were performing a creep movement [2].

However, as was mentioned above, the amount of this sand naturally changes depending upon the size of the crevices. Therefore, one may conclude that Bagnold's opinion is incorrect.

Next, when we calculate the mean value of L , we find that:

$$\begin{aligned}\bar{L} &= \int_0^{\infty} xy(x)dx \\ &= -\frac{1}{G_0} \left[|x F(x)|_0^{\infty} - \int_0^{\infty} F(x)dx \right] \\ &= \frac{1}{G_0} \int_0^{\infty} F(x)dx\end{aligned} \quad \left| \quad \frac{/112}{\quad} \right|$$

On the other hand, according to (10.6), we have

$$Q = G_0 \bar{L}$$

Therefore, comparing both equations, we find that

$$Q = \int_0^{\infty} F(x)dx$$

This is the basic principle of the horizontal type sand collector, which was already described in section 10.

13. CONCLUSIONS

Research was performed on flying sand caused by wind, concentrating on dune sand. Based on considerations of the suspension of sand grains caused by wind turbulence and on actual observations of flying sand, the conclusion was reached that flying sand is not a diffusion phenomenon caused by wind turbulence. From this standpoint, wind turbulence was omitted in the discussion of sand movement in the air. Based on considerations of the friction stress operating on the sand surface, the relationships between the

mean values of the total flow rate, etc., and the friction velocity of the wind were derived theoretically. The accelerated flying sand at the forefront of the sand surface was also discussed, and it was possible to explain the interactions between wind and sand. These theoretical results were proved to be correct in wind tunnel and outdoor experiments.

Next, flying sand was regarded as an aggregate motion of numerous grains of sand, and this was treated statistically. It was possible to obtain theoretically the density distribution of sand grains in the flying sand layer as well as the flying sand distribution. It was established that these theoretical results coincide well with the experiments. Finally, the method of seeking the flight distance distribution of the grains of sand was discussed, and typical examples of the experimental results were given.

In conclusion, the writer expresses his gratitude to Professor Sanji Kawada, who kindly provided guidance and encouragement throughout to this research. He also wishes to thank Messrs. Kan'ichi Hirooka and Teruo Nakano, who assisted him in the experiments.

REFERENCES

1. Exner, F. M. Sitzungsber. Mathem.-naturw. Kl., Wien Ab., Vol. IIa, 1928, p. 137.
2. Bagnold, R. A. Proc. Roy. Soc., London, Vol. A, 1936, p. 157.
3. Bagnold, R. A. Proc. Roy. Soc., London, Vol. A, 1937, p. 163.
4. Bagnold, R. A. Proc. Roy. Soc., London, Vol. A, 1938, p. 167.
5. Prandtl, L. Zeitschr. V.D.I., 1933, p. 77.
6. Taylor, G. I. Proc. Roy. Soc., London, Vol. A, 1938, p. 164.
7. Lamb, H. Hydrodynamics, Sixth Ed.
8. Schiller, L. Handb. Exp.-phys., Vol. VI, 2 Teil.
9. Jeffreys, H. Camb. Phil. Soc., 1929, p. 25.
10. Davis, R. F. Engineering, 1935, p. 140.
11. White, C. M. Proc. Roy. Soc., London, Vol. A, 1940, p. 174.
12. Chepil, W. S. Soil Science, 1945, p. 60 and 1946, p. 61.
13. Watson, G. N. Theory of Bessel Function, 1922.

Translated for National Aeronautics and Space Administration under Contract No. NASw-2035, by SCITRAN, P. O. Box 5456, Santa Barbara, California 93108.